RAA 2020 Vol. **20** No. **12**, 191(5pp) doi: 10.1088/1674-4527/20/12/191

http://www.raa-journal.org *http://iopscience.iop.org/raa*

***R**esearch in*
***A**stronomy and*
***A**strophysics*

LETTERS

The timing residual patterns due to pulsar acceleration

Yi Xie[1] and Li-Chun Wang[1,2]

[1] School of Science, Jimei University, Xiamen 361021, China; *xieyi@jmu.edu.cn*
[2] Physics Experiment Center, Jimei University, Xiamen 361021, China; *wanglc@jmu.edu.cn*

Received 2020 February 6; accepted 2020 October 20

Abstract The form of timing residuals due to errors in pulsar spin period P and its derivative $\dot{P}$, in positions, as well as in proper motions, has been well presented for decades in the literature. However, the residual patterns due to errors in the pulsar acceleration have not been reported previously, while a pulsar in the Galaxy or a globular cluster (GC) will be unavoidably accelerated. The coupling effect of the pulsar transverse acceleration and the Römer delay on timing residuals is simulated in this work. The results demonstrate that the residuals due to the effect can be identified by the oscillation envelopes of the residuals. It is also shown that the amplitude of the residuals due to the effect is usually relatively small, however, it may probably be observable for pulsars distributed in the vicinity of the core of a nearby GC.

Key words: stars: neutron, stars: rotation, pulsars: general, surveys

1 INTRODUCTION

Pulsars are very stable rotators with rapid radio pulses. Pulsar timing analysis is based on the measurement of the precise pulse times of arrival (TOAs) at the telescope. The remarkable TOAs period stability opens up a wide range of potential applications, e.g. establishing a pulsar-based time standard (Kaspi et al. 1994; Hobbs et al. 2012), detecting nanohertz-frequency gravitational waves (GWs) (e.g. Jenet et al. 2004; Sesana et al. 2008; Verbiest et al. 2009; Lee et al. 2011; NANOGrav Collaboration et al. 2015; Desvignes et al. 2016; Reardon et al. 2016; Burke-Spolaor et al. 2019), developing pulsar-based navigation techniques (Sheikh et al. 2006; Deng et al. 2013; Zheng et al. 2019), improving the solar system ephemeris (e.g. Champion et al. 2010), studying various scientific targets such as the interstellar medium and the solar wind (You et al. 2007, 2012), etc. Using the TEMPO[1] or TEMPO2[2] programs, the TOAs can be transformed to the solar system barycenter which approximates an inertial frame. The spin period and period derivatives, the position and the proper motion of the pulsar can also be obtained by fitting the TOAs to a pulsar timing model (Hobbs et al. 2006; Edwards et al. 2006). The differences between the observed and the model predicted TOAs are known as timing residuals.

Fitting errors in the parameters of the timing model will be revealed by systematic trends in the timing residuals. The patterns of these residuals due to various errors in the timing model, such as in pulsar spin period P and its derivative $\dot{P}$, in positions and in proper motions have been well presented for decades in the literature (Lyne & Graham-Smith 2012). It was also noticed that the fitted period derivative may be different from its intrinsic value if the pulsar is accelerating in the gravitational field of the Galaxy or a globular cluster (GC) (Phinney 1992, 1993). Some authors further studied the gravitational effects of the dark matter halo on pulsar timing (Schneider 1990; Larchenkova & Doroshenko 1995; Fargion & Conversano 1996; Seto & Cooray 2007; Siegel et al. 2007; Baghram et al. 2011; Bramante & Linden 2014; Nomura et al. 2020). Though the magnitudes of the timing parameters of the accelerating pulsar have been widely investigated, the residual patterns for errors in pulsar acceleration have not been reported previously. Phinney (1992, 1993) showed that if a pulsar experiences a component of acceleration a_l along the line of sight, the observed period derivative is generally related to the intrinsic value by $\dot{P}_{\rm obs} = \dot{P}_{\rm int} + (a_l/c)P$. Thus one may infer that its residual pattern should be identical with that due to an error in the spin period derivative $\dot{P}$. However, up to date, the residual pattern due to an error in the transverse acceleration of a pulsar is still unknown.

Edwards et al. (2006) estimated the magnitude of the acceleration terms, for both the Galactic gravitational

[1] `http://www.pulsar.princeton.edu/tempo`
[2] `http://www.atnf.csiro.au/research/pulsar/tempo2`

acceleration ($a \sim 10^{-11}$ m s^{-2}) and the greater acceleration in GCs ($a \sim 10^{-8}$ m s^{-2}), for all pulsars in the Australia Telescope National Facility (ATNF) Pulsar Catalogue[3] (Manchester et al. 2005). They affirmed that only the radial acceleration term and Shklovskii term involving a exceed 1 nanosecond (ns) for a 20-yr observing campaign. Thus, all the other acceleration terms are neglected in TEMPO2 (see section 2.3 of Edwards et al. 2006). However, as we demonstrate later (in subsection 2.1), the amplitudes, due to the coupling effect of the pulsar transverse acceleration and the Römer delay, could be clearly larger than the maximum allowable systematic error of the TEMPO ($\sim$ 100 ns) and TEMPO2 ($\sim$ 1 ns) programs, and may also be detectable for pulsars in the nearest GCs, and thus need more investigations.

In this work, we present a realistic simulation of the residual pattern for a pulsar with transverse acceleration, and its possible applications are also discussed. The organization of this paper is as follows. The magnitude of the coupling effect and its influences on pulsar timing parameters are described in Section 2. The simulations and results are detailed in Section 3. Finally, we summarize the main results in Section 4.

2 METHODS

2.1 The Coupling Effect of the Pulsar Transverse Acceleration and the Römer Delay

The issue is essentially attributed to the geometric propagation delay (Edwards et al. 2006). The displacement vector ($\boldsymbol{R}$) from the observatory to an isolated pulsar is the sum of the position of the pulsar ($\boldsymbol{R_0}$), the displacement of the pulsar ($\boldsymbol{k}$) in the time elapsed since epoch $t_{\rm pos}$ and the barycentric position of the observatory ($\boldsymbol{r}$)

$$\boldsymbol{R} = \boldsymbol{R_0} + \boldsymbol{k} - \boldsymbol{r} = \boldsymbol{R_0} + \boldsymbol{k}_\parallel - \boldsymbol{r}_\parallel + \boldsymbol{k}_\perp - \boldsymbol{r}_\perp. \quad (1)$$

where the radial and transverse components are denoted by subscripts, i.e. $i_\parallel = \boldsymbol{i}\cdot\boldsymbol{R_0}/|\boldsymbol{R_0}|$ and $\boldsymbol{i}_\perp = \boldsymbol{i} - i_\parallel \boldsymbol{R_0}/|\boldsymbol{R_0}|$, and $\boldsymbol{i}$ is an arbitrary vector. Neglecting terms of the order of $|\boldsymbol{R_0}|^{-3}$, the following relation is obtained

$$|\boldsymbol{R}| = |\boldsymbol{R_0}| + k_\parallel - r_\parallel + \frac{1}{|\boldsymbol{R_0}|}\left(\frac{|\boldsymbol{k}_\perp|^2}{2} + \frac{|\boldsymbol{r}_\perp|^2}{2} - \boldsymbol{k}_\perp\cdot\boldsymbol{r}_\perp\right) \left(1 - \frac{k_\parallel}{|\boldsymbol{R_0}|} + \frac{r_\parallel}{|\boldsymbol{R_0}|}\right). \quad (2)$$

The terms in the first pair of parentheses are the Shklovskii effect, annual parallax and annual proper motion. The displacement $\boldsymbol{k}$ may be broken into the first and second derivatives (Edwards et al. 2006)

$$\boldsymbol{k} = \boldsymbol{\mu}|\boldsymbol{R_0}|(t^{\rm psr} - t_{\rm pos}) + \frac{\boldsymbol{a}}{2}(t^{\rm psr} - t_{\rm pos})^2, \quad (3)$$

where $\boldsymbol{\mu}$ is the velocity divided by the distance, $\boldsymbol{a}$ is the acceleration vector and $t^{\rm psr}$ is the proper time measured at the pulsar.

Edwards et al. (2006) assumed that $\boldsymbol{k} = \boldsymbol{\mu}|\boldsymbol{R_0}|(t^{\rm psr} - t_{\rm pos})$, and except for radial acceleration term and Shklovskii term, all the other acceleration terms are neglected in TEMPO2. Consequently, TEMPO2 does not include the coupling effect of the pulsar transverse acceleration and the Römer delay, i.e. for the annual proper motion term of Equation (2),

$$\frac{\boldsymbol{k}_\perp\cdot\boldsymbol{r}_\perp}{|\boldsymbol{R_0}|} = \boldsymbol{\mu}_\perp\cdot\boldsymbol{r}_\perp(t^{\rm psr} - t_{\rm pos}) + \frac{\boldsymbol{a}_\perp\cdot\boldsymbol{r}_\perp}{2|\boldsymbol{R_0}|}(t^{\rm psr} - t_{\rm pos})^2, \quad (4)$$

the second term on the right hand side is neglected (see also equation 24 of Edwards et al. 2006). Thus, the magnitude of the timing residual of the coupling effect can be expressed as

$$\Delta'_{\rm R\odot} = -\frac{\boldsymbol{a}_\perp\cdot\boldsymbol{r}_\perp}{2|\boldsymbol{R_0}|c}(t^{\rm psr} - t_{\rm pos})^2, \quad (5)$$

where c is the speed of light. If one takes $a_\perp \sim 5\times 10^{-8}$m s^{-2}, $R_0 \sim 1$ kpc and $r_\perp \sim 1$ AU as an estimation for the case of a pulsar in a GC, the amplitude of the residual is about 160 ns for a 20-yr observing campaign.

2.2 The Effects on Pulsar Timing Residuals

As described above, the coupling effect of the pulsar transverse acceleration and the Römer delay is not included in the timing model of TEMPO2. Applying ecliptic coordinates (λ, β) and assuming a circular Earth orbit that is centered on the Sun, the Römer time delay is given by (Lyne & Graham-Smith 2012)

$$t_{\rm R} = t_\oplus \cos(\omega t - \lambda)\cos\beta, \quad (6)$$

where $t_\oplus \simeq 498.7$ s is the light travel time from the Sun to the Earth, $\omega \simeq 2.0\times 10^{-7}$ s^{-1} is the angular velocity of the Earth in its orbit, λ and β are the ecliptic longitude and latitude of the pulsar respectively, and $\lambda = -\pi/2$ and $\beta = \pi/4$ are assumed in the following calculations.

A neglected transverse acceleration $a_\perp$ will induce errors in the coordinates, i.e. $\delta\lambda = [v_\perp(t^{\rm psr} - t_{\rm pos}) + \frac{1}{2}a_\perp(t^{\rm psr} - t_{\rm pos})^2]\sin\xi/d_0$ and $\delta\beta = [v_\perp(t^{\rm psr} - t_{\rm pos}) + \frac{1}{2}a_\perp(t^{\rm psr} - t_{\rm pos})^2]\cos\xi/d_0$, in which $v_\perp$ is the transverse velocity, ξ ($= \pi/4$ is taken in the following calculations) is the angle between the acceleration and the longitude line, and d_0 is the distance between the pulsar and the Earth. The errors give rise to periodic timing errors

$$\begin{aligned}\delta t_{\rm R} = {} & t_\oplus \sin[\omega(t^{\rm psr} - t_{\rm pos}) - \lambda]\cos\beta\delta\lambda \\ & - t_\oplus \cos[\omega(t^{\rm psr} - t_{\rm pos}) - \lambda]\sin\beta\delta\beta.\end{aligned} \quad (7)$$

The corresponding error of a pulse phase is $\delta\phi = 2\pi\nu\delta t_{\rm R}$, in which ν is the rotation frequency of the pulsar.

[3] https://www.atnf.csiro.au/research/pulsar/psrcat/

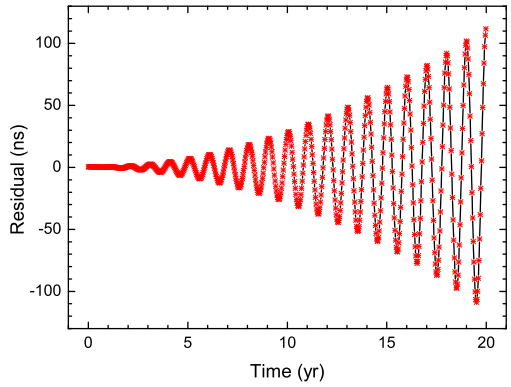

Fig. 1 The simulated timing residual due to the coupling effect of the pulsar transverse acceleration and the Römer delay. The transverse acceleration $a_\perp = 5 \times 10^{-8}\ \mathrm{m\,s^{-2}}$ and the distance $d_0 = 1\ \mathrm{kpc}$ are adopted in the simulations.

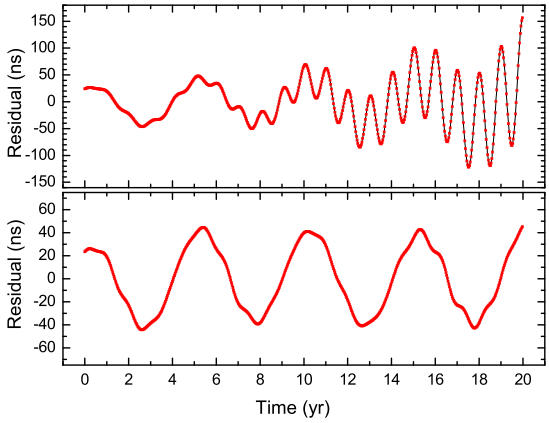

Fig. 2 The simulated timing residuals with three oscillation modes and the transverse acceleration of a pulsar. *Upper panel*: the residual in fitting the phase with Eq. (9). *Bottom panel*: the residual in fitting the phase with Eq. (11).

3 SIMULATIONS

3.1 The Residual Pattern

We firstly develop a phenomenological spin-down model to describe the pulse phase evolution, so that the model can be a tool for simulating the TOA data. Assuming the pure magnetic dipole radiation in vacuum is the braking mechanism for a pulsar's spin-down (Lorimer & Kramer 2004), the pulse phase evolution can be described as

$$\ddot{\phi}(t) + \frac{8\pi^2 B^2 R^6 \sin\theta^2}{3c^3 I}\dot{\phi}(t)^3 = 0, \tag{8}$$

where B is the strength of the dipole magnetic field at the surface of the neutron star, and R ($\simeq 10^6$ cm), I ($\simeq 10^{45}\ \mathrm{g\,cm^2}$) and θ ($\simeq \pi/2$) are the radius, moment of inertia and angle of magnetic inclination, respectively. Solving Equation (8) and incorporating the coupling effect into the phase evolution, one can get the theoretical phase function $\Phi_{\rm T}(t) = \phi(t) + \delta\phi$.

We take the moderate initial values of $P_0 = 0.005$ s and $\dot{P}_0 = 1.0 \times 10^{-20}\ \mathrm{s\,s^{-1}}$ for a millisecond pulsar (MSP). The transverse acceleration $a_\perp = 5 \times 10^{-8}\mathrm{m\,s^{-2}}$ is assumed for the gravitational field of the GC (Phinney 1993). We assume a certain time interval $\Delta t_{\rm int} = 10^6$ s between each two nearby TOAs to simulate the observed TOA series (Xie et al. 2015; Xie & Zhang 2019). Since the rotational period is nearly constant, the pulsar spin frequency ν, and its derivatives $\dot{\nu}$ and $\ddot{\nu}$ can be obtained by fitting the TOA series to third order (cubic term) of its Taylor expansion over a time span $T_{\rm s}$,

$$\Phi(t) = \Phi_0 + \nu(t-t_0) + \frac{1}{2}\dot{\nu}(t-t_0)^2 + \frac{1}{6}\ddot{\nu}(t-t_0)^3. \tag{9}$$

The pulsar period $P = 1/\nu$ and its derivative $\dot{P} = -\dot{\nu}/\nu^2$ are quoted in place of ν and $\dot{\nu}$ respectively. Here we are not concerned with the relativistic frame transformation between observatory proper time and pulsar proper time, thus $t = t^{\rm psr}$ and $t_0 = t_{\rm pos}$ are simply taken in the simulation. A timing residual is conventionally defined as

$$(\mathrm{Residual}) \equiv \frac{\Phi_{\rm T}(t) - \Phi(t)}{2\pi\nu}. \tag{10}$$

The results are displayed in Figure 1. One can clearly see the residual pattern with oscillation period of one year. *The oscillation envelope of the residual due to velocity error consists of two straight lines, while two parabolic curves correspond to the acceleration origin. This characteristic may be utilized to identify the transverse acceleration of a pulsar.* The root-mean-square (rms) of the residual due to the effect is about 100 ns, which is consistent with the estimate of Equation (5). Considering the larger distance d_0 for most of the GCs, the rms of practical residuals (inversely proportional to d_0) would be much smaller, and probably be drowned by other timing residuals. Hence the pattern formed by the residuals has not been reported.

The pulsar transverse acceleration cannot be well determined if the oscillation is drowned by other timing residuals. Based on the simulated envelopes of the residual curves, we speculate that the pulse phase with the annual effects may be characterized by

$$\Phi(t) = \Phi_0 + \nu(t-t_0) + \frac{1}{2}\dot{\nu}(t-t_0)^2 + \frac{1}{6}\ddot{\nu}(t-t_0)^3 + \dot{\nu}'(t-t_0)^2\cos[\omega(t-t_0)+\lambda'], \tag{11}$$

in which $\dot{\nu}'$ and λ' are free parameters. $\dot{\nu}'$ is responsible for the residual due to the coupling effect, and ω is the angular velocity of the Earth in its orbit. We perform again the residual simulation with the same parameters, but fit the

phase sequences with Equation (11). The magnitude of the simulated residuals is fairly low ($\ll 1$ ns), which means the effect can be described well with Equation (11), at least for the case that the timing residuals are uncorrelated in pulsar timing.

If the annual effect correlates with "red noises", which consist of low-frequency structures in timing residuals, it may cause some errors in estimating the parameters of the timing model and their uncertainties (Coles et al. 2011). For this case, we firstly construct a phenomenological model for the pulsar timing residual with multi-periodic oscillations, and the pulse phase evolution can be rewritten in the following form

$$\ddot{\phi} + \frac{8\pi^2 B^2 R^6 \sin\theta^2}{3c^3 I} G(t)^2 \dot{\phi}^3 = 0, \qquad (12)$$

in which $G(t) = 1 + \sum_{i=1}^{N} k_i \sin(2\pi \frac{t}{T_i})$, and k_i and T_i are the magnitude and period for the i-th oscillation, respectively. Then, we simulate the "red noises" for three oscillation modes, and the period for two of them is about one year. Thus in the simulations, the three oscillation modes with $k_1 = k_2 = k_3 = 10^{-4}$, $T_1 = 0.9$ yr, $T_2 = 1.1$ yr and $T_3 = 5.0$ yr are adopted (see Zhang & Xie 2013; Xie et al. 2015, for more details about the simulation). For the annual effect, we also take $a_\perp = 5 \times 10^{-8}\ \mathrm{m\,s^{-2}}$. The simulated residuals in fitting the phase with Equation (9) and Equation (11) are shown in the upper and lower panels of Figure 2, respectively. By comparing the two residuals, one can see that the annual effect of the transverse acceleration is fully separated out by Equation (11), since the curve in the bottom panel overlaps completely with the residual curve for the same oscillation modes but not the annual effect.

3.2 Residual Amplitudes of Pulsars in GCs

In the above simulations, $d_0 = 1$ kpc and $a_\perp = 5 \times 10^{-8}\ \mathrm{m\,s^{-2}}$ are assumed. However in more practical cases, distances for many GCs are usually $\gtrsim 5$ kpc, thus inducing residuals with amplitude of only tens of nanoseconds, which is relatively small, even though these pulsars have the highest timing precision (e.g., Perera et al. 2019). However, a pulsar's transverse acceleration due to the GC's mean field differs from its location with respect to the center of gravity (CoG) and the GC geometry.

We define the plane running through the CoG and perpendicular to our line-of-sight as O, the core radius of the GC as r_c, the impact parameter for each pulsar from the CoG as $R'_\perp$, the line-of-sight position going perpendicularly through O as l and the pulsar's spherical radius r' ($= \sqrt{R'^2_\perp + l^2}$). Then the cluster acceleration felt at any given radius out from the core can be written as

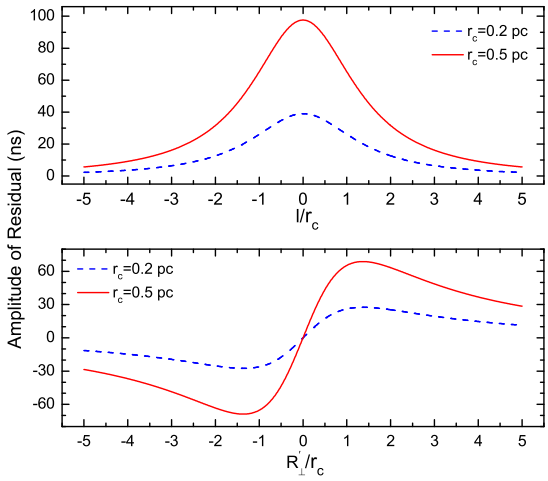

Fig. 3 The amplitudes of timing residuals due to the coupling effect of the pulsar transverse acceleration and the Römer delay, for pulsars in a GC for 20-yr observing campaign. *Upper panel*: the residual amplitude with respect to l, and $R'_\perp = r_c$ is taken in the calculation. *Bottom panel*: the residual amplitude with respect to $R'_\perp$, and $l = r_c$ is assumed.

(Prager et al. 2017)

$$a_r(r') = -4\pi G \rho_c r_c^3 r'^{-2} [\sinh^{-1}(\frac{r'}{r_c}) - \frac{r'}{r_c\sqrt{1+(r'/r_c)^2}}] \qquad (13)$$

where $a_r(r')$ is the mean-field acceleration and ρ_c is the core density. The King density profile which most strongly sets the GC potential (King 1962),

$$\rho(r') \simeq \rho_c [1 + (r'/r_c)^2]^{-\frac{3}{2}}, \qquad (14)$$

is included in the model. We get the transverse acceleration $a_\perp$ by projecting the acceleration $a_r(r')$ along the transverse direction by a factor of $R'_\perp/r'$. Substituting typical values of $\rho_c = 10^6\ M_\odot\ \mathrm{pc^{-3}}$ and $d_0 = 5$ kpc for the GC, and using Equation (5), we obtain the amplitude of the residuals for various l or $R'_\perp$, as depicted in Figure 3. As expected, the amplitudes are very sensitive to r_c, and actually proportional to the mass of the core. The results also imply that the residuals due to the coupling effect may probably be observed, particularly for those pulsars which are distributed in the vicinity of big cores and located near the O plane.

The amplitudes of the residuals presented in Figure 1 and Figure 3 do not depend on the initial values of pulsar spin parameters (e.g. P and $\dot{P}$), and thus are universal for different pulsars. The simulations for MSPs or normal pulsars in the Galaxy with $g_G = 10^{-10}\ \mathrm{m\,s^{-2}}$ are also performed, and we found that the acceleration is small and has little influence on pulsar timing.

4 SUMMARY

We simulated the timing residuals of a pulsar due to the coupling effect of the transverse acceleration and the Römer delay, for a 20-yr observing campaign. It is found that the envelopes of the residuals due to the pulsar acceleration are two parabolic curves, which may be used to identify the transverse acceleration of a pulsar. Even if drowned by other timing residuals, they can also be modeled well and separated out with Equation (11). However, the annual effect on pulsar timing is usually relatively small: for pulsars in the Galactic field, the acceleration due to the Galactic potential is of the order of about $g_{\rm G} = 10^{-10}\ {\rm m\,s^{-2}}$, which induces timing residual < 1 ns. Only for these pulsars in GCs, this effect is possibly needed. We calculated the amplitudes for pulsars distributed around the cores of GCs, and the results imply that the coupling effect may probably be observed for pulsars located near the O plane in close clusters. We expect to gain more details on the timing residuals and a much deeper understanding of GC dynamics applying future larger samples of MSPs with higher precision data, to be acquired by China's Five-hundred-meter Aperture Spherical radio-Telescope (FAST) and the future Square Kilometre Array (SKA).

Acknowledgements We thank Dr. Jian-ping Yuan for valuable discussions. We thank the anonymous referee for comments and suggestions that led to a significant improvement in this manuscript. This work is supported by the National Natural Science Foundation of China (Grant Nos. 11803009 and 11603009), and by the Natural Science Foundation of Fujian Province (Grant Nos. 2018J05006, 2018J01416 and 2016J05013).

References

Baghram, S., Afshordi, N., & Zurek, K. M. 2011, Phys. Rev. D, 84, 043511
Bramante, J., & Linden, T. 2014, Phys. Rev. Lett., 113, 191301
Burke-Spolaor, S., Taylor, S. R., Charisi, M., et al. 2019, A&A Rev., 27, 5
Champion, D. J., Hobbs, G. B., Manchester, R. N., et al. 2010, ApJL, 720, L201
Coles, W., Hobbs, G., Champion, D. J., Manchester, R. N., & Verbiest, J. P. W. 2011, MNRAS, 418, 561
Deng, X. P., Hobbs, G., You, X. P., et al. 2013, Advances in Space Research, 52, 1602
Desvignes, G., Caballero, R. N., Lentati, L., et al. 2016, MNRAS, 458, 3341
Edwards, R. T., Hobbs, G. B., & Manchester, R. N. 2006, MNRAS, 372, 1549
Fargion, D., & Conversano, R. 1996, in The Dark Side of the Universe; Experimental Efforts and Theoretical Framework, eds. R. Bernabei, & A. Incicchitti, 252
Hobbs, G. B., Edwards, R. T., & Manchester, R. N. 2006, MNRAS, 369, 655
Hobbs, G., Coles, W., Manchester, R. N., et al. 2012, MNRAS, 427, 2780
Jenet, F. A., Lommen, A., Larson, S. L., & Wen, L. 2004, ApJ, 606, 799
Kaspi, V. M., Taylor, J. H., & Ryba, M. F. 1994, ApJ, 428, 713
King, I. 1962, AJ, 67, 471
Larchenkova, T. I., & Doroshenko, O. V. 1995, A&A, 297, 607
Lee, K. J., Wex, N., Kramer, M., et al. 2011, MNRAS, 414, 3251
Lorimer, D. R., & Kramer, M. 2004, Handbook of Pulsar Astronomy, 4 (UK: Cambridge Univ. Press)
Lyne, A., & Graham-Smith, F. 2012, Pulsar Astronomy (Francis Graham-Smith, Cambridge, UK: Cambridge Univ. Press)
Manchester, R. N., Hobbs, G. B., Teoh, A., & Hobbs, M. 2005, AJ, 129, 1993
NANOGrav Collaboration, Arzoumanian, Z., Brazier, A., et al. 2015, ApJ, 813, 65
Nomura, K., Ito, A., & Soda, J. 2020, European Physical Journal C, 80, 419
Perera, B. B. P., DeCesar, M. E., Demorest, P. B., et al. 2019, MNRAS, 490, 4666
Phinney, E. S. 1992, Philosophical Transactions of the Royal Society of London Series A, 341, 39
Phinney, E. S. 1993, in Astronomical Society of the Pacific Conference Series, 50, Structure and Dynamics of Globular Clusters, eds. S. G. Djorgovski, & G. Meylan, 141
Prager, B. J., Ransom, S. M., Freire, P. C. C., et al. 2017, ApJ, 845, 148
Reardon, D. J., Hobbs, G., Coles, W., et al. 2016, MNRAS, 455, 1751
Schneider, J. 1990, in New and Exotic phenomena, eds. O. Fackler, & J. Tran Thanh Van, 301
Sesana, A., Vecchio, A., & Colacino, C. N. 2008, MNRAS, 390, 192
Seto, N., & Cooray, A. 2007, ApJL, 659, L33
Sheikh, S. I., Pines, D. J., Ray, P. S., et al. 2006, Journal of Guidance Control Dynamics, 29, 49
Siegel, E. R., Hertzberg, M. P., & Fry, J. N. 2007, MNRAS, 382, 879
Verbiest, J. P. W., Bailes, M., Coles, W. A., et al. 2009, MNRAS, 400, 951
Xie, Y., & Zhang, S.-N. 2019, ApJ, 880, 123
Xie, Y., Zhang, S.-N., & Liao, J.-Y. 2015, RAA (Research in Astronomy and Astrophysics), 15, 963
You, X. P., Hobbs, G., Coles, W. A., et al. 2007, MNRAS, 378, 493
You, X. P., Coles, W. A., Hobbs, G. B., & Manchester, R. N. 2012, MNRAS, 422, 1160
Zhang, S.-N., & Xie, Y. 2013, International Journal of Modern Physics D, 22, 1360012
Zheng, S. J., Zhang, S. N., Lu, F. J., et al. 2019, ApJS, 244, 1